PROCEEDINGS OF SPIE

SPIEDigitalLibrary.org/conference-proceedings-of-spie

Placenta accreta spectrum and hysterectomy prediction using MRI radiomic features

Leitch, Ka'Toria, Shahedi, Maysam, Dormer, James, Do, Quyen, Xi, Yin, et al.

Ka'Toria Leitch, Maysam Shahedi, James D. Dormer, Quyen N. Do, Yin Xi, Matthew A. Lewis, Christina L. Herrera, Catherine Y. Spong, Ananth J. Madhuranthakam, Diane M. Twickler, Baowei Fei, "Placenta accreta spectrum and hysterectomy prediction using MRI radiomic features," Proc. SPIE 12033, Medical Imaging 2022: Computer-Aided Diagnosis, 120331I (4 April 2022); doi: 10.1117/12.2611587

SPIE.

Event: SPIE Medical Imaging, 2022, San Diego, California, United States

Placenta Accreta Spectrum and Hysterectomy Prediction Using MRI Radiomic Features

Ka'Toria Leitch [1], Maysam Shahedi [1], James D. Dormer [1], Quyen N. Do [2], Yin Xi [2,3], Matthew A. Lewis [2], Christina L. Herrera [4], Catherine Y. Spong [4], Ananth J. Madhuranthakam [2], Diane M. Twickler [2,4], Baowei Fei [1,2]

[1]Department of Bioengineering, The University of Texas at Dallas, Richardson, TX
[2]Department of Radiology, [3]Department of Clinical Science, [4]Department of Obstetrics and Gynecology, The University of Texas Southwestern Medical Center, Dallas, TX

ABSTRACT

In women with placenta accreta spectrum (PAS), patient management may involve cesarean hysterectomy at delivery. Magnetic resonance imaging (MRI) has been used for further evaluation of PAS and surgical planning. This work tackles two prediction problems: predicting presence of PAS and predicting hysterectomy using MR images of pregnant patients. First, we extracted approximately 2,500 radiomic features from MR images with two regions of interest: the placenta and the uterus. In addition to analyzing two regions of interest, we dilated the placenta and uterus masks by 5, 10, 15, and 20 mm to gain insights from the myometrium, where the uterus and placenta overlap in the case of PAS. This study cohort includes 241 pregnant women. Of these women, 89 underwent hysterectomy while 152 did not; 141 with suspected PAS, and 100 without suspected PAS. We obtained an accuracy of 0.88 for predicting hysterectomy and an accuracy of 0.92 for classifying suspected PAS. The radiomic analysis tool is further validated, it can be useful for aiding clinicians in decision making on the care of pregnant women.

Keywords: Placenta accreta spectrum (PAS), radiomics, magnetic resonance imaging (MRI), uterus, machine learning, pregnant, hysterectomy

1. INTRODUCTION

During pregnancy, the placenta and uterus must work in harmony to ensure optimal living conditions for the mother and her developing fetus. Placenta accreta spectrum (PAS) is a pathological condition in which the placenta invades into the uterine wall and thus fails to separate after delivery. The occurrence of PAS is steadily rising[1], due to increasing number of cesarean deliveries and can have significant maternal morbidity[2] including emergency hysterectomy, blood transfusion, and intensive care admission. Timely diagnosis of PAS allows planning and the necessary support to reduce the chance of maternal morbidity[3].

Radiomics is an emerging machine learning approach in the field of radiology aiming to extract a high-dimensional set of features from clinical data for quantitative analysis of the data[4]. In previous work, nearly 40% of radiomic features were found to be consistent between expert segmented and deep-learning segmented placenta and uterus volumes[5-7]. Hysterectomy was predicted with an area under the curve (AUC) of 0.69 for manually segmented data, and 0.78 for deep-learning segmented data using radiomic features, magnetic resonance imaging (MRI) data, and placenta and uterus segmentation masks. Another group achieved 0.94 accuracy when predicting placental invasion on T2-Weighted MRI using a mixture of radiomics and deep learning[8]. Color doppler ultrasound is the first line of clinical PAS diagnosis. Using ultrasound, significant differences ($P < 0.05$) are found between pregnant women that require hysterectomy and those who do not[9]. This work investigates PAS and hysterectomy prediction using MRI radiomics.

Medical Imaging 2022: Computer-Aided Diagnosis, edited by Karen Drukker, Khan M. Iftekharuddin, Hongbing Lu, Maciej A. Mazurowski, Chisako Muramatsu, Ravi K. Samala, Proc. of SPIE Vol. 12033, 120331I · © 2022 SPIE · 1605-7422 · doi: 10.1117/12.2611587

2. METHODS

2.1 MRI Acquisition

We performed an IRB approved review of 241 pregnancies. Images were acquired on a 1.5T MR scanner (Avanto, Siemens Healthcare, Erlangen, Germany). Half Fourier single shot turbo spin echo (HASTE) T2-weighted axial imaging sequence covering the entire gravid uterus was evaluated. Each image volume had 28 to 52 two-dimensional (2D) transverse slices. Each MRI slice was configured to be 256 × 256 pixels. The axial image slice spacing is 7.0 mm and the pixels are isotropic across slices. In plan resolution ranges from 1.05 × 1.05 mm^2 to 1.72 × 1.72 mm^2.

2.2 Database

Of the 241 pregnant women, 100 were normal and 141 were PAS-suspected; of these, 89 required hysterectomy and 52 did not. For each patient, an expert radiologist manually segmented the uterine cavity and placenta. As a result, each patient had two corresponding masks, or regions of interest. In addition, we were provided data regarding the suspected presence of PAS and corresponding hysterectomy treatment outcome status.

2.3 Image Processing

For each patient, the MR images were dilated using 5, 10, 15, and 20 mm in MATLAB (MathWorks, Inc., Natick, MA). Figure 1 illustrates the effects of dilation on the placenta mask (A) and uterus mask (B). The placenta mask (A) is dilated to mimics PAS by simulating the invasion of the placenta into the myometrium. Typically, the myometrium is approximately 7 mm thick during pregnancy[10]. Therefore, dilation from 0-10 mm resembles normal thickness, 10-20 represents the various stages of PAS.

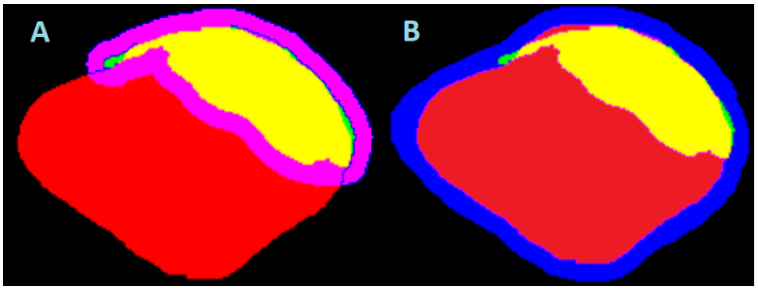

Figure 1. Example changes in area from one patient slice at 10 mm dilation, where the uterus mask is red and the placenta mask is yellow. (A) The pink area denotes the dilation of the placenta mask by 10 mm. (B) The blue are denotes the dilation of the uterus mask by 10 mm.

2.4 Radiomic Feature Extraction and Selection

Both non-dilated and dilated MRI were loaded into PyRadiomics where 2,463 unique features were extracted. These features are the result of several image filters, feature class, and feature setting parameters being manipulated. The parameters that were tested are summarized in feature extraction settings section. All radiomic feature definitions were established by the Imaging Biomarker Standardization Initiative (IBSI)[11].

After feature extraction, radiomic feature selection was performed. The purpose of feature selection is to avoid issues presented by high dimensionality, algorithm performance, noisy or ambiguous data, and replicability of the study[12]. The goal of feature selection is to identify the relationship between the radiomic feature(s) and the presence of PAS or hysterectomy[13]. Three feature selection methods were implemented: analysis of variance (ANOVA), LASSO, and Ridge Regression. These feature selection methods can be categorized into filter and embedded tools. ANOVA is a filter method. Filter methods are useful due to their quick computation time and

intolerance to overfitting. LASSO and Ridge Regression are examples of embedded feature selection tools. These methods work by combining filter and wrapper methods into a learning algorithm[14-17].

2.5 Machine Learning

Seventeen machine learning algorithms were tested for each of the three feature extraction methods and five dilation groups (0, 5, 10, 15, 20 mm), for a total of 255 combinations. All machine learning algorithms were implemented using the python scikit-learn package with their default parameters[12]. Classifiers were trained using an independent training set. The predictive performance was evaluated based on an independent testing set using accuracy analysis. Both the independent training and testing sets were randomly selected on a patient basis. Each dilation group was tested within the group. For example, a 5 mm dilated training set was used to train the algorithm for the 5 mm dilated testing set. In the study, 157 patients were used for training, 24 patients for validation, and 60 patients for testing. No patient overlaps occurred between the training and testing groups.

3. RESULTS

PAS was classified with 92% accuracy using both uterus and placenta masks (Table 1). Uterus mask resulted in 92% accuracy without dilation, and placenta mask required 20 mm dilation. For the placenta mask, the feature selection algorithm was ANOVA and the algorithm was Extra Gradient Boost Classifier. For the uterus mask, the feature selection and the algorithms were the same.

Table 1. Accuracy as a relationship between mask type and dilation for predicting PAS on the testing set.

	Dilation (mm)				
	None	**5**	**10**	**15**	**20**
Placenta	0.88	0.88	0.87	0.90	**0.92**
Uterus	**0.92**	0.86	0.82	0.87	0.85

Hysterectomy clinical outcome was classified with 88% accuracy using the placenta mask without dilation on the whole test set including the normal cases (Table 2). To obtain 88% with the placenta mask, LASSO feature selection tool was used in conjunction with the Gradient Boost Classifier.

The most important features for predicting PAS using the placenta mask are voxel-based calculated volume (hereafter called ‘voxel-based volume’), maximum 3D diameter, and mesh volume (i.e., the volume that is represented by a surface mesh). The most important features for predicting PAS using the uterus mask are voxel-based volume, mesh volume, and minor axis length. The most important features for predicting hysterectomy using the placenta mask are voxel-based volume, maximum 3D diameter, and mesh volume. Table 3 summarizes these features where voxel-based volume is the most frequently chosen feature among predicting PAS and hysterectomy treatment response. Voxel-based volume is calculated by multiplying the number of voxels in the region of interest by the volume of a single voxel.

Table 2. Accuracy as a relationship between mask type and dilation for predicting hysterectomy on the testing set (including the normal cases).

	Dilation (mm)				
	None	**5**	**10**	**15**	**20**
Placenta	**0.88**	0.85	0.80	0.85	0.83
Uterus	0.83	0.80	0.82	0.82	0.85

Table 3. Top three radiomic features chosen for each prediction (PAS or hysterectomy).

PAS (Placenta Mask)	**PAS (Uterus Mask)**	**Hysterectomy**
Voxel-based Volume	Voxel-based Volume	Voxel-based Volume
Maximum 3D Diameter	Mesh Volume	Maximum 3D Diameter
Mesh Volume	Minor Axis Length	Mesh Volume

4. DISCUSSION & CONCLUSION

We developed an MRI-based radiomic method for PAS and hysterectomy prediction. PAS was independently classified with an accuracy of 0.92 without image augmentation of the uterus mask. Hysterectomy clinical outcome was classified with an accuracy of 0.88 when using the placenta mask without image augmentation. The voxel-based volume feature was found to be important for the prediction.

The major limitation of this study is the small data set. The number of patients (N=241) may not be sufficient to generalize the applicability of this study in a clinical environment. Although we implemented an independent testing set, we cannot conclude that this data is representative of all cases that may be presented. If we had access to a larger dataset, it is likely that the model presented here would be more universal in its applicability. For hysterectomy prediction, we tested the algorithm on a test set with both PAS and normal cases. In future work, we are going to follow a decision tree and predict the hysterectomy using the cases that were classified as PAS during the first step. This approach is more compatible with the current clinical workflow and could be helpful to have a better evaluation over the whole workflow. We also anticipate a higher hysterectomy prediction rate using this approach.

In addition to the voxel-based volume feature, the data suggest that maximum 3D diameter, mesh volume, and minor axis length are connected to determining PAS and hysterectomy. Voxel-based volume combined with maximum 3D diameter can be related to the sphericity of the region of interest. For a specific 3D diameter value, the closer the volume is to a sphere, the greater the volume. Mesh volume and minor axis length follow similar patterns. When taking a closer look at the placenta radiomic features, we found that hysterectomy and PAS positive individuals were more likely to have features corresponding to spherical placentas. With this understanding, we may be able to conclude that placenta shapes that are more spherical tend to develop PAS and require hysterectomy. More research must be done in order to make this assertion. However, this study has demonstrated promise for using radiomics and MRI to aid in early detection of PAS and prepare patients for potential hysterectomy planning.

ACKNOWLEDGMENTS

This research was supported in part by the U.S. National Institutes of Health (NIH) grants (R01CA156775, R01CA204254, R01HL140325, and R21CA231911) and by the Cancer Prevention and Research Institute of Texas (CPRIT) grant RP190588.

REFERENCES

[1] Jauniaux, E., Kingdom, J. C., and Silver, R. M., "A comparison of recent guidelines in the diagnosis and management of placenta accreta spectrum disorders," Best Practice & Research Clinical Obstetrics & Gynaecology, 72, 102-116 (2021).

[2] Matsuzaki, S., Mandelbaum, R. S., Sangara, R. N., McCarthy, L. E., Vestal, N. L., Klar, M., Matsushima, K., Amaya, R., Ouzounian, J. G., and Matsuo, K., "Trends, characteristics, and outcomes of placenta accreta spectrum: a national study in the United States," American Journal of Obstetrics and Gynecology, 225(5), 534. e1-534. e38 (2021).

[3] Afshar, Y., Dong, J., Zhao, P., Li, L., Wang, S., Zhang, R. Y., Zhang, C., Yin, O., Han, C. S., and Einerson, B. D., "Circulating trophoblast cell clusters for early detection of placenta accreta spectrum disorders," Nature communications, 12(1), 1-14 (2021).

[4] Yip, S. S., and Aerts, H. J., "Applications and limitations of radiomics," Physics in Medicine & Biology, 61(13), R150 (2016).

[5] Xi, Y., Shahedi, M., Do, Q. N., Dormer, J., Lewis, M. A., Fei, B., Spong, C. Y., Madhuranthakam, A. J., and Twickler, D. M., "Assessing reproducibility in magnetic resonance (MR) radiomics features between deep-learning segmented and expert manual segmented data and evaluating their diagnostic performance in pregnant women with suspected placenta accreta spectrum (PAS)." 11597, 115972P.

[6] Shahedi, M., Dormer, J. D., TT, A. D., Do, Q. N., Xi, Y., Lewis, M. A., Madhuranthakam, A. J., Twickler, D. M., and Fei, B., "Segmentation of uterus and placenta in MR images using a fully convolutional neural network." 11314, 113141R.

[7] Shahedi, M., Spong, C. Y., Dormer, J. D., Do, Q. N., Xi, Y., Lewis, M. A., Herrera, C., Madhuranthakam, A. J., Twickler, D. M., and Fei, B., "Deep learning-based segmentation of the placenta and uterus on MR images," Journal of Medical Imaging, 8(5), 054001 (2021).

[8] Shao, Q., Xuan, R., Wang, Y., Xu, J., Ouyang, M., Yin, C., and Jin, W., "Deep learning and radiomics analysis for prediction of placenta invasion based on T2WI," Mathematical Biosciences and Engineering, 18(5), 6198-6215 (2021).

[9] Yule, C. S., Lewis, M. A., Do, Q. N., Xi, Y., Happe, S. K., Spong, C. Y., and Twickler, D. M., "Transvaginal Color Mapping Ultrasound in the First Trimester Predicts Placenta Accreta Spectrum: A Retrospective Cohort Study," Journal of Ultrasound in Medicine, 40(12), 2735-2743 (2021).

[10] Buhimschi, C. S., Buhimschi, I. A., Malinow, A. M., and Weiner, C. P., "Myometrial thickness during human labor and immediately post partum," American journal of obstetrics and gynecology, 188(2), 553-559 (2003).

[11] Zwanenburg, A., Leger, S., Vallières, M., and Löck, S., "Image biomarker standardisation initiative," arXiv preprint arXiv:1612.07003, (2016).

[12] Pedregosa, F., Varoquaux, G., Gramfort, A., Michel, V., Thirion, B., Grisel, O., Blondel, M., Prettenhofer, P., Weiss, R., and Dubourg, V., "Scikit-learn: Machine learning in Python," the Journal of machine Learning research, 12, 2825-2830 (2011).

[13] Dhal, P., and Azad, C., "A comprehensive survey on feature selection in the various fields of machine learning," Applied Intelligence, 1-39 (2021).

[14] Hamon, J., [Optimisation combinatoire pour la sélection de variables en régression en grande dimension: Application en génétique animale] Université des Sciences et Technologie de Lille-Lille I, (2013).

[15] Yu, L., and Liu, H., "Feature selection for high-dimensional data: A fast correlation-based filter solution." 856-863.
[16] Phuong, T. M., Lin, Z., and Altman, R. B., "Choosing SNPs using feature selection." 301-309.
[17] Saghapour, E., Kermani, S., and Sehhati, M., "A novel feature ranking method for prediction of cancer stages using proteomics data," PLoS One, 12(9), e0184203 (2017).

APPENDIX: FEATURE EXTRACTION SETTINGS

Extraction Settings	weightingNorm = Manhattan distances = 1:1:10 interpolator 1:1:10 padDistance = 3 preCrop = True, False resegmentMode = relative resegmentShape = True, False correctMask = True False kernelRadius = 0:1:9 maskedKernel = True, False
Image Filters	LoG Wavelet Square SquareRoot Logarithm Exponential Gradient LBP3D
Image Filter Settings	LoG settings: sigma = 0.25:0.25:2.5 Gradient settings: gradientUseSpacing = True Wavelet settings: start level = 0:1:9 Wavelet settings: level = 5, 10, 1, 20, 30, 40, 50, 60, 70, 80 Wavelet settings: wavelet = all possible wavelets
Feature Settings	voxelArrayShift = 0:2000 symmetricalGLCM = True, False gldm_a = 0:.25:0.25:2.5